Article

Journal of the Brazilian Chemical Society

https://dx.doi.org/10.21577/0103-5053.20230139

J. Braz. Chem. Soc. **2024**, *35*, 2, e-20230139 , 1-12

Design, Synthesis, and Molecular Docking Studies of New Quinoline-Thiazole Hybrids, Potential Leads in the Development of Novel Antileukemic Agents

*Victor Facchinetti,[a,b] Claudia Regina B. Gomes,[a] Karoline C. L. Aboud,[a] Rodolfo G. Fiorot,[b] Guilherme G. C. de Carvalho,[c] Carlos Roberto K. Paier,[c] Claudia do Ó Pessoa,[c] Anne Caroline C. Gomes,[d] Marcus Vinícius N. de Souza *,[a] and Thatyana R. A. Vasconcelos *,[b]*

[a]*Instituto de Tecnologia em Fármacos (Farmanguinhos), Fundação Oswaldo Cruz, 21041-250 Rio de Janeiro-RJ, Brazil*

[b]*Instituto de Química, Universidade Federal Fluminense, 24020-141 Niterói-RJ, Brazil*

[c]*Departamento de Fisiologia e Farmacologia, Universidade Federal do Ceará, 60430-275 Fortaleza-CE, Brazil*

[d]*Instituto Federal de Educação, Ciência e Tecnologia do Rio de Janeiro, Campus Realengo, 21715-000 Rio de Janeiro-RJ, Brazil*

This work describes the multigram-scale synthesis of the building-block N^1-(7-chloroquinolin-4-yl)ethane-1,2-diamine via sonochemistry and its use in the synthesis of seven new quinoline-thiazole hybrids endowed with interesting anticancer activity. Target compounds were planned based on the drugs chloroquine and primaquine and the desired thiazoles were obtained through the Hantzsch thiazole synthesis, without the use of catalysts, by reacting key intermediate 1-(2-((7-chloroquinolin-4-yl)amino)ethyl)thiourea, obtained in two-steps from N^1-(7-chloroquinolin-4-yl)ethane-1,2-diamine, with different 2-bromoacetophenones. The novel molecules were assessed against four different leukemia cell lines (HL60, K562, KASUMI-1, and KG-1) plus normal fibroblasts (L929), using the 3-(4,5-dimethyl-2-thiazol)-2,5-diphenyl-2*H*-tetrazolium bromide (MTT) assay, and showed, overall, a high cytotoxic profile, but with interesting selectivity index, especially against K562 cells (1.89 to 5.50), when compared to standard doxorubicin (3.51). Docking studies suggest that all tested derivatives are able to interact with BCR-ABL1 tyrosine kinase enzyme, and, therefore, these molecules may be promising leads against chronic myeloid leukemia.

Keywords: quinolines, thiazoles, antileukemic, design, synthesis

Introduction

Cancer is a complex disease that varies extensively in its form, being one of the main causes of death worldwide. The Global Cancer Observatory project (GLOBOCAN) calculates 9.96 million deaths by cancer in 2020, and the World Health Organization (WHO) estimates a total burden of 30.2 million cases by 2040 with at least 16.3 million deaths.[1] Nowadays, blood cancer responds for 10% of all new cancer cases.[2]

According to the Leukemia and Lymphoma Society,[2] every 3 min one person is diagnosed with a blood cancer in the United States. Among them, leukemia, a type of cancer caused by an abnormal proliferation of white blood cells, responds to roughly 35% of all cases and is the most common cancer in children.[2] This disease is classified by how quickly it progresses and by the type of cell involved, such as acute myeloid leukemia (AML), chronic myeloid leukemia (CML), acute lymphoid leukemia (ALL), and chronic lymphoid leukemia (CLL).[3] The discovery of the BCR-ABL gene, which is found in 90% of patients with CML, and the advent of imatinib (Figure 1) to treat this disease, have shown that it is possible to use molecules targeting specific pathways in cancer, but cell-cycle nonspecific drugs are still widely used in therapy.[4-6]

In this context, the quinoline scaffold became an important motif in cancer drug development after the discovery of the anticancer activity of quinolinic alkaloids, such as camptothecin and neratinib, and the ability of

*e-mail: mvndesouza@gmail.com; thatyanavasconcelos@id.uff.br
Editor handled this article: Brenno A. D. Neto

quinoline derivatives in inhibiting topoisomerase I and various protein kinases (Figure 1).[7-9]

Moreover, the importance of the thiazole ring in drug development has become clear after the advent of relevant small molecules such as dasatinib, thiazofurin, sudoxicam, and famotidine (Figure 2).[10,11]

Our research group has vast experience in the synthesis of quinolines with potential anticancer activity. Therefore, molecules **1**, containing the quinoline and thiazole backbones, were planned from the structure of the antimalarials chloroquine and primaquine and some previously reported structures (**2**, **3**, and **4**) (Figure 3).[12-14] It is important to mention that primaquine and chloroquine are known to act as chemosensitizers against some multidrug-resistant cancer cell lines.[15,16] Ethylenediamine was chosen as the linker to grant some flexibility to the proposed structures and for its capacity to act as a sequestering agent for metal ions in cancer cells.[17,18] All synthesized molecules were assessed against the chronic myeloid leukemia cell line K562, and three acute myeloid leukemia cell lines, HL60 (acute promyelocytic leukemia), Kasumi-1 (acute myeloblastic leukemia), and KG-1 (acute myelogenous leukemia), to evaluate their anticancer potential.

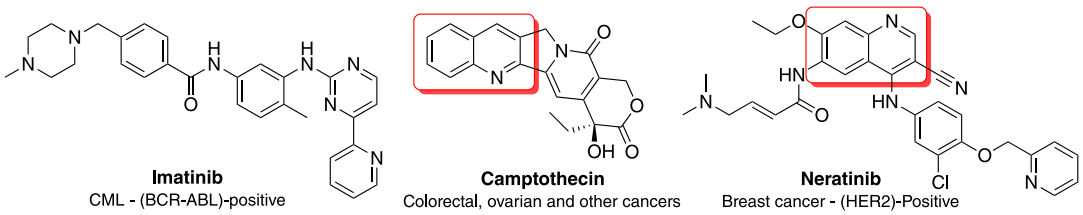

Figure 1. Imatinib, camptothecin, and neratinib, molecules with anticancer activity.

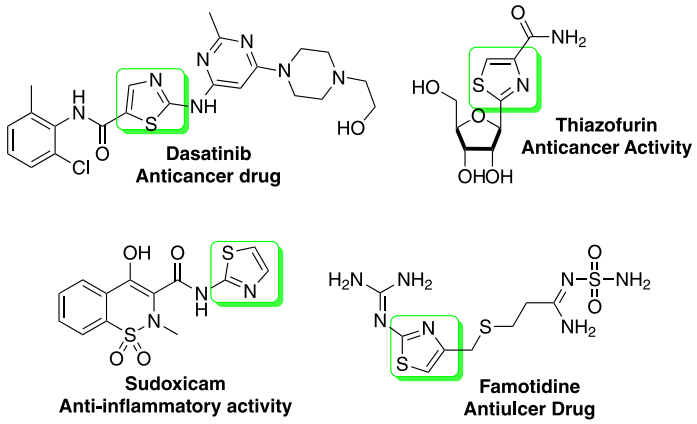

Figure 2. Small molecules endowed with biological activity containing the thiazole motif.

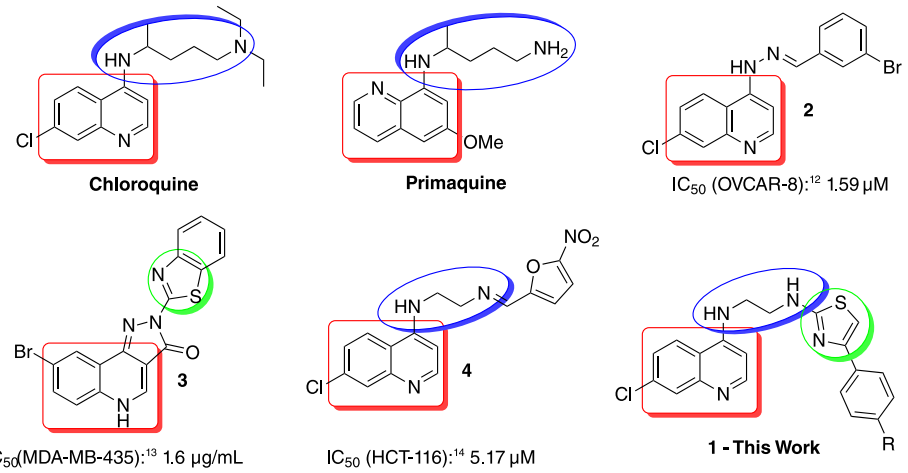

Figure 3. Proposed molecules **1** and some previously reported[12-14] structures with anticancer activity. IC_{50}: half maximal inhibitory concentration.

Experimental

Chemistry

Reactions were monitored by thin-layer chromatography (TLC) on silica-gel precoated F254 Merck plates (Darmstadt, Germany) visualized under UV light (254-366 nm). Melting points were determined using an MQAPF-302 (MicroQuímica Ltd, Palhoça, Brazil) instrument and are uncorrected. A multiwave Eco-sonics (Indaiatuba, Brazil) QR750 ultrasonic generator (20 kHz, 750 W) equipped with a converter and a titanium oscillator (horn, diameter = 4 mm) was used for the ultrasonic irradiation. Nuclear magnetic resonance (NMR) spectra were obtained using 400 or 500 MHz Bruker (Billerica, United States of America) AC spectrometers in dimethyl sulfoxide (DMSO-d_6) or methanol (CD_3OD) (Cambridge Isotope Laboratories Inc., Tewksbury, USA), as the deuterated solvent. Chemical shifts (δ) are reported in parts *per* million (ppm) relative to tetramethylsilane (TMS), which was used as an internal standard. Infrared (IR) spectra were obtained using a Thermo Scientific (Waltham, United States of America) Nicolet 6700 spectrometer, and frequencies are expressed in cm^{-1}. High-resolution mass spectra (HRMS) ESI-TOF (electrospray ionization, time of flight) in positive ion mode were acquired on a Bruker (Billerica, United States of America) compact-TOF. All chemicals and solvents were obtained from commercial suppliers and used without further purification. Sodium hydroxide was obtained from Merck (Darmstadt, Germany). Ammonium thiocyanate and benzoyl chloride were obtained from VETEC (Duque de Caxias, Brazil). All bromoacetophenones, ethylenediamine, and 4,7-dichloroquinoline were obtained from Sigma-Aldrich (Burlington, USA). Finally, ethyl ether was obtained from Tedia (Fairfield, USA), acetone from Sciavicco (Sabará, Brazil), and ethanol from Proquimios (Rio de Janeiro, Brazil).

Procedure for the synthesis of *N*^{1}-(7-chloroquinolin-4-yl) ethane-1,2-diamine (**5**)

Methodology 1

Ethylenediamine (9 mL) and 4,7-dichloroquinoline (12 mmol, 2.4 g) were added to a 50 mL round-bottom flask and allowed to react for 2 h under reflux until the complete consumption of 4,7-dichloroquinoline was observed (TLC). The reaction mixture was poured over ice and the resulting solid was filtered, washed with 20 mL of water, and, finally, 20 mL of ethyl ether to furnish **5**.

Methodology 2

A 50 mL glass flask was charged with ethylenediamine (15 mL) and 4,7-dichloroquinoline (12 mmol, 2.4 g). The reaction mixture was submitted to ultrasound irradiation (US) for 30 min (2 × 15 min) at 90% maximum power output until all 4,7-dichloroquinoline was consumed (TLC). The crude product was isolated by pouring the reaction mixture over ice and purified as in methodology 1, by washing with 20 mL of water and 20 mL of ethyl ether to furnish **5**.

N^1-(7-Chloroquinolin-4-yl)ethane-1,2-diamine (**5**)

Gray solid; yield: 90% (heat), 97% (US); mp 140-142 ºC; IR (ATR) ν / cm^{-1} 3466 (NH), 3352 (NH), 3297 (NH); ^{1}H NMR (400.00 MHz, MeOD) δ 8.36 (d, *J* 5.6 Hz, 1H, H2), 8.11 (d, *J* 9.0 Hz, 1H, H5), 7.78 (d, *J* 2.2 Hz, 1H, H8), 7.40 (dd, *J* 9.0, 2.2 Hz, 1H, H6), 6.57 (d, *J* 5.7 Hz, 1H, H3), 3.45 (t, *J* 6.4 Hz, 2H, CH_2), 2.98 (t, J 6.4 Hz, 2H, CH_2); ^{13}C NMR (100.0 MHz, MeOD) δ 152.9 (C2), 152.5 (Ph), 149.7 (Ph), 136.4 (C7), 127.6 (C8), 126.1 (Ph), 124.4 (Ph), 118.9 (C4a), 99.8 (C3), 46.3 (CH_2), 40.9 (CH_2); HRMS (ESI) *m/z*, calcd. for $C_{11}H_{12}ClN_3$ $[M + H]^+$: 222.0798, found: 222.0798.

Procedure for the synthesis of key intermediate **7**

Benzoyl isothiocyanate was formed *in situ*, in a 50 mL round-bottom flask, from the reaction of ammonium thiocyanate (4 mmol) and benzoyl chloride (1 mmol, added dropwise over 5 min) in refluxing acetone (15 mL, 30 min), under magnetic stirring. A solution of intermediate **5** (1 mmol) in acetone (10 mL) was then added to the round-bottom flask containing the freshly formed benzoyl isothiocyanate, and the development of a yellow color in the reaction medium was promptly observed. The mixture was kept under reflux and stirred for 2 h until the complete consumption of intermediate **5** (TLC). The reaction mixture was poured over ice, yielding crude product **6a**, which was filtered, dissolved in 10 mL of ethanol, and allowed to react with 1 mL aqueous 1 M NaOH under reflux for 20 min. Key intermediate **7** was furnished after evaporation followed by extraction with ethyl acetate (3 × 20 mL) and used in the next step without further purification.

General procedure for the synthesis of compounds **1a-1g**

Key intermediate **7** was added to a 25 mL round-bottom flask and dissolved in 10 mL of acetone. The respective bromoacetophenone **8a-8g** (1 mmol) was added to the flask and the reaction mixture was kept under reflux and magnetic stirring for 30 min, until the precipitation of the product, as HBr salt, was observed. The precipitate was

filtered and washed with 10 mL of acetone to afford pure products **1a-1g** in 20-25% global yield.

*N*¹-(7-Chloroquinolin-4-yl)-*N*²-(4-(4-methoxyphenyl)thiazol-2-yl)ethane-1,2-diamine hydrobromide (**1a**)

Yellow solid; global yield: 22%; mp 210-213 ºC; IR (ATR) ν / cm^{-1} 3225 (NH), 1607 (C=N), 1213 (C-N); ^{1}H NMR (400.00 MHz, DMSO-d_6) δ 14.34 (s, 1H, NH), 9.71 (s, 1H, NH), 8.58-8.55 (m, 1H, H6), 8.54 (d, *J* 7.1 Hz, 1H, H2), 8.03 (brs, 1H, H8), 7.94 (t, *J* 5.4 Hz, 1H, NH), 7.64-7.61 (m, 3H, H2'' and H5), 7.02 (d, *J* 7.2 Hz, 1H, H3), 6.91 (d, *J* 8.9 Hz, 2H, H3''), 6.86 (s, 1H, H5'), 3.84-3.77 (m, 5H, C$\underline{H}_2$A and OC$\underline{H}_3$), 3.67 (dd, *J* 11.4, 5.7 Hz, 2H, CH_2B); ^{13}C NMR (100.0 MHz, DMSO-d_6) δ 167.9 (C2'), 158.5 (C4''), 155.7 (C4), 149.4 (C4'), 142.5 (C2), 138.4 (C8a), 137.7 (C7), 127.5 (C1''), 126.7 (C2''), 126.5 (C5), 125.7 (C6), 118.8 (C8), 115.5 (C4a), 113.6 (C3''), 99.1 (C5'), 98.6 (C3), 55.0 (OCH_3), 42.7 (CH_2A), 42.0 (CH_2B); HRMS (ESI) *m/z*, calcd. for $C_{21}H_{19}ClN_4OS$ $[M + H]^+$: 411.1046, found: 411.1069.

*N*¹-(7-Chloroquinolin-4-yl)-*N*²-(4-(4-fluorophenyl)thiazol-2-yl) ethane-1,2-diamine hydrobromide (**1b**)

Yellow solid; global yield: 21%; mp 143-145 ºC; IR (ATR) ν /cm^{-1} 1612 (C=N), 1208 (C-N); ^{1}H NMR (500.00 MHz, MeOD) δ 8.34 (d, *J* 7.2 Hz, 1H, H2), 8.03 (d, *J* 9.1 Hz, 1H, H5), 7.70-7.62 (m, 3H, Ph, H8), 7.16 (dd, *J* 9.1, 2.0 Hz, 1H, H6), 7.06 (t, *J* 8.8 Hz, 2H, Ph), 6.99 (d, *J* 7.2 Hz, 1H, H3), 6.72 (s, 1H, H5'), 3.87 (s, 4H, C$\underline{H}_2$); ^{13}C NMR (125.0 MHz, MeOD) δ 171.3 (C2'), 163.9 (d, *J* 243.8 Hz, C4''), 158.3 (C4), 150.8 (C4'), 143.7 (C2), 140.9 (C7), 140.0 (C8a), 132.9 (d, *J* 2.9 Hz, C1''), 129.0 (d, *J* 8.1Hz, C2''), 128.4 (C6), 126.2 (C5), 120.2 (C8), 117.1 (C4a), 116.4 (d, *J* 21.9, C3''), 102.2 (C5'), 100.1 (C3), 46.3 ($\underline{C}H_2$), 43.5 ($\underline{C}H_2$); HRMS (ESI) *m/z*, calcd. for $C_{20}H_{16}ClFN_4S$: 399.0846 $[M + H]^+$, found: 200.0582 $[M + 2H]^{2+}$, 399.1044.

*N*¹-(7-Chloroquinolin-4-yl)-*N*²-(4-(4-toluyl)thiazol-2-yl) ethane-1,2-diamine hydrobromide (**1c**)

Yellow solid; global yield: 25%; mp 151-152 ºC; IR (ATR) ν / cm^{-1} 3226 (NH), 1606 (C=H), 1211 (CN); ^{1}H NMR (500.00 MHz, MeOD) δ 8.32 (d, *J* 7.2 Hz, 1H, C2), 7.99 (d, *J* 9.0 Hz, 1H, C5), 7.67 (d, *J* 1,9 Hz, 1H, H8), 7.55 (d, *J* 8.0 Hz, 2H, Ph), 7.16 (d, *J* 7.9 Hz, 2H, Ph), 6.98-6.92 (m, 2H, H6 and H3), 6.70 (s, 1H), 3.89 (m, 2H, C$\underline{H}_2$), 3.86-3.81 (m, 2H, C$\underline{H}_2$) 2.37 (s, 3H, C$\underline{H}_3$); ^{13}C NMR (125.0 MHz, MeOD) δ 171.6 (C2'), 158.2 (C4), 151.9 (C4'), 143.7 (C2), 140.8 (C7), 140.0 (C8a), 138.8 (C1''), 133.8 (Ph), 130.3 (Ph), 128.3 (C6), 127.3 (Ph), 126.3 (C5), 120.2 (C8), 116.9 (C4a), 101.9 (C5'), 100.0 (C3), 46.9 ($\underline{C}H_2$), 43.6 ($\underline{C}H_2$), 21.4 ($\underline{C}H_3$); HRMS (ESI) *m/z*, calcd. for $C_{21}H_{19}ClN_4S$: 395.1097 $[M + H]^+$, found: 198.0702 $[M + 2H]^{2+}$, 395.1097.

*N*¹-(7-Chloroquinolin-4-yl)-*N*²-(4-(4-nitrophenyl)thiazol-2-yl) ethane-1,2-diamine hydrobromide (**1d**)

Yellow solid; global yield: 20%; mp 250 ºC (d); IR (ATR) ν / cm^{-1} 3184 (NH), 1120 (CN); ^{1}H NMR (400.00 MHz, MeOD) δ 8.40 (d, *J* 7.2 Hz, 1H, H2), 8.23-8.18 (m, 2H, H3''), 8.14 (d, *J* 9.1 Hz, 1H, H5), 7.83-7.77 (m, 2H, H3''), 7.69 (d, *J* 2.0 Hz, 1H, H8), 7.39 (dd, *J* 9.1, 2.1 Hz, 1H, H6), 7.15 (s, 1H, H5''), 7.05 (d, *J* 7.2 Hz, 1H, H3), 3.95-3.91 (m, 4H, CH_2); ^{13}C NMR (100.0 MHz, DMSO-d_6) δ 168.3 (C2'), 155.8 (C4), 147.3 (C4'), 145.8 (C4''), 142.7 (C2), 140.3 (C7), 138.3 (C8a), 137.8 (Ph), 126.6 (C6), 126.0 (Ph), 125.6 (C5), 118.7 (C8), 115.5 (C4a), 106.3 (C5'), 98.6 (C3), 42.8 ($\underline{C}H_2$), 41.9 ($\underline{C}H_2$); HRMS (ESI) *m/z*, calcd. for $C_{20}H_{16}ClN_5O_2S$: 426.0791 $[M + H]^+$, found: 426.0790.

*N*¹-(7-Cloroquinolin-4-il)-*N*²-(4-(4-clorofenil)tiazol-2-il) ethane-1,2-diamine hydrobromide (**1e**)

Yellow solid; global yield: 20%; mp 260 ºC (d); IR (ATR) ν / cm^{-1} 3347 (NH), 3223 (NH), 1606 (C=N), 1213 (CN); ^{1}H NMR (400.00 MHz, MeOD) δ 8.47 (d, *J* 7.1 Hz, 1H, H2), 8.42 (d, *J* 9.1 Hz, 1H, H5), 7.86 (d, *J* 2.0 Hz, 1H, H8), 7.67-7.64 (m, 2H, Ph), 7.62 (dd, *J* 8,9, 1,8 Hz, 1H, H6), 7.49 (d, *J* 8.7 Hz, 2H, Ph), 7.09-7.02 (m, 2H, H3 and H5'), 4.02-3.98 (m, 2H, C$\underline{H}_2$), 3.97-3.92 (m, 2H, C$\underline{H}_2$); ^{13}C NMR (100.0 MHz, DMSO-d_6) δ 168.3 (C2'), 155.7 (C4), 142.6 (C2), 138.4 (C7), 137.8 (C8a), 131.9 (C4'), 129.2 (C1''), 128.3 (Ph), 128.0 (Ph), 127.2 (C6), 126.6 (Ph), 125.7 (C5), 118.8 (C8), 115.5 (C4a), 102.3 (C5'), 98.5 (C3) 42.5 ($\underline{C}H_2$), 42.3 ($\underline{C}H_2$); HRMS (ESI) *m/z*, calcd. for $C_{20}H_{16}Cl_2N_4S$: 415.0551 $[M + H]^+$, found: 415.0545.

*N*¹-(7-Chloroquinolin-4-yl)-*N*²-(4-(4-bromophenyl)thiazol-2-yl)ethane-1,2-diamine hydrobromide (**1f**)

Yellow solid; global yield: 25%; mp 153-154 ºC; IR (ATR) ν / cm^{-1} 3203 (NH), 1611 (C=N), 1208 (CN); ^{1}H NMR (500.00 MHz, MeOD) δ 8.34 (d, *J* 7.2 Hz, 1H, H2), 8.01 (d, *J* 9.1 Hz, 1H, H5), 7.67 (d, *J* 1.9 Hz, 1H, H8), 7.53 (d, *J* 8.6 Hz, 2H, Ph), 7.46 (d, *J* 8.6 Hz, 2H, Ph), 7.16 (dd, *J* 9.1, 2.0 Hz, 1H, H6), 7.00 (d, *J* 7.2 Hz, 1H, H3), 6.81 (s, 1H, H5'), 3.92-3.82 (m, 4H, C$\underline{H}_2$); ^{13}C NMR (125.0 MHz, MeOD) δ 171.2 (C2'), 158.2 (C4), 150.5 (C4'), 143.5 (C2), 140.8 (C7), 139.9 (C8a), 135.4 (C1''), 132.6 (Ph), 128.8 (Ph), 128.3 (C6), 126.0 (C5), 122.2 (Ph), 120.1 (C8), 117.0 (C4a), 103.1 (C5'), 100.0 (C3), 46.2 ($\underline{C}H_2$), 43.4 ($\underline{C}H_2$); HRMS (ESI) *m/z*, calcd. for $C_{20}H_{16}BrClN_4S$: 461.0025 $[M + H]^+$, found: 461.0049.

*N*¹-(7-Chloroquinolin-4-yl)-*N*²-(4-phenylthiazol-2-yl)ethane-1,2-diamine hydrobromide (**1g**)

Yellow solid; global yield: 25%; mp 211-212 ºC; IR (ATR) ν / cm^{-1} 3273 (NH), 3202 (NH), 1612 (C=N), 1215 (CN); ^{1}H NMR (400.00 MHz, MeOD) δ 8.33 (d, *J* 7.2 Hz, 1H, H2), 7.99 (d, *J* 9.1 Hz, 1H, H5), 7.70-7.67 (m, 2H, Ph), 7.66 (d, *J* 1.8 Hz, 1H, H8), 7.38-7.27 (m, 3H, Ph), 7.00-6.95 (m, 2H, H6 e H3), 6.78 (s, 1H, H5'), 3.93-3.88 (m, 2H, C$\underline{H}_2$), 3.85-3.83 (m, 2H, C$\underline{H}_2$); ^{13}C NMR (100.0 MHz, MeOD) δ 171.5 (C2'), 158.0 (C4), 151.8 (C4'), 143.7 (C2), 140.6 (C7), 140.0 (C8a), 136.4 (C1''), 129.6 (Ph), 128.7 (Ph), 128.2 (C6), 127.2 (Ph), 126.1 (C5), 120.2 (C8), 116.9 (C4a), 102.6 (C5'), 99.9 (C3), 46.7 ($\underline{C}H_2$), 43.4 ($\underline{C}H_2$); HRMS (ESI) *m/z*, calcd. for $C_{20}H_{17}ClN_4S$: 381.0941 $[M + H]^+$, found: 381.0924.

Biology

Compounds were tested for cytotoxic activity in cell culture *in vitro* using several human cancer cell lines obtained from the National Cancer Institute (NCI, Bethesda, USA). Cytotoxicity was checked on four cancer cell lines: Kasumi-1 (acute myeloblastic leukemia), KG-1 (acute myelogenous leukemia), HL-60 (acute promyelocytic leukemia), and K562 (chronic myelogenous leukemia).

Murine fibroblast immortalized cell line (L929) was used as the control lineage. All culture media (Dulbecco's Modified Eagle Medium (DMEM) for L929 and Roswell Park Memorial Institute (RPMI) for HL-60, K562, Kasumi-1, and KG-1) were supplemented with 10% fetal bovine serum (except KG-1 and Kasumi-1 which were supplemented with 20% fetal bovine serum (FBS) and 2 mM L-glutamine), 100 IU mL^{-1} penicillin, 100 µg mL^{-1} streptomycin at 37 ºC with 5% CO_2. In cytotoxicity experiments, cells were plated in 96-well plates (0.1×10^6 cells well^{-1} for L929 and 0.3×10^6 cells well^{-1} for Kasumi-1, KG-1, HL-60, and K562). All compounds tested were dissolved in DMSO. The final concentration of DMSO in the culture medium was kept constant (0.1%, v/v). Doxorubicin was used as the positive control, and negative control groups received the same amount of vehicle (DMSO). The cell viability was determined by the reduction of the yellow dye 3-(4,5-dimethyl-2-thiazol)-2,5-diphenyl-2*H*-tetrazolium bromide (MTT) to a blue formazan product as described by Mosmann.[19,20] At the end of the incubation time (72 h), the plates were centrifuged and the medium was replaced by fresh medium (200 µL) containing 0.5 mg mL^{-1} MTT. Three hours later, the MTT formazan product was dissolved in DMSO (150 µL) and the absorbance was measured using a multiplate reader (Spectra Count, Packard, Ontario, Canada). The influence of the compound on cell proliferation and survival was quantified as the percentage of control absorbance of the reduced dye at 550 nm. The results were obtained by nonlinear regression for all cell lines from three independent experiments. All cell treatments were performed with three replicates. All cells were mycoplasma-free.[20]

Molecular docking

Computational methods

Molecular docking calculations were performed with the BCR-ABL1 Tyrosine Kinase (Protein Data Bank, PDB ID: 3QRJ),[21] using AutoDock Vina software.[22,23] The structures of the synthesized molecules were constructed in MarvinSketch,[24] and their protonated states were adjusted to the plasmatic pH (7.4). The structures had their geometries fully optimized at the Gaussian09 software,[25] with the default convergence criteria, at the Density Functional Theory (DFT) level, using B3LYP/6-31+G(d).[26] These structures were characterized as minimum energy points on the potential energy surfaces by frequency calculation (with all the values positive). To proceed to the docking calculations, we kept only the polar hydrogen atoms of the receptor and the small molecules (co-crystallized ligand, rebastinib, and our synthesized molecules). This approach, known as the united-atom model, simplifies the docking calculation by merging the nonpolar hydrogen atoms to the carbon atoms to which they are bonded. Thus, it reduces the overall number of atoms with little sacrifice of accuracy, since other interactions are more relevant in the inhibition of the BCR-ABL1 Tyrosine Kinase, such as hydrogen bonds with the Met318 amino acid residue.[21]

The docking protocol was established by setting the scanning space (Grid Box) centered on the co-crystallized ligand (Cartesian coordinates x; y; z of 5.153; –14.078; 27.236 and dimensions of 11, 22, and 11 Å, respectively), which was validated by superimposing the docked pose to the co-crystallized ligand. The necessary inputs to perform the redocking have been added to the Supplementary Information section. Discovery Studio Visualizer 2019 software was used to evaluate the interactions established between ligands and the amino acids residues from the docking calculations.[27]

Results and Discussion

Synthesis

Besides being interested in the construction of novel molecules endowed with biological activity against cancer and tropical diseases, our research group has also

developed many new methodologies for the synthesis of building blocks on a multigram scale, especially by using sonochemistry to speed up reactions or to obtain increased yields.[28,29] In this context, the nucleophilic aromatic substitution reaction of 4,7-dichloroquinoline with ethylenediamine (Scheme 1) has been previously reported by many research groups, including our own.[30] Usually, ethylenediamine is used as the solvent and the reaction mixture is kept under reflux (116 °C) for a few hours, furnishing the desired product in high yields after easy work-up. To evaluate the potential use of sonochemistry in this transformation, we replicated the reaction conditions previously reported by our group,[30] in a multigram scale (2.4 g, 12 mmol of 4,7-dichloroquinoline, under reflux) and compared it to our newly developed sonochemistry methodology (Scheme 1). The desired building block **5** was obtained in excellent yields by using both methodologies, but, remarkably, the ultrasound synthesis was 4× faster (30 min) than the classic protocol (2 h) and afforded the desired product in quantitative yields (97%). This new methodology may apply to other similar nucleophilic aromatic substitutions and the scope of this reaction is currently being investigated.

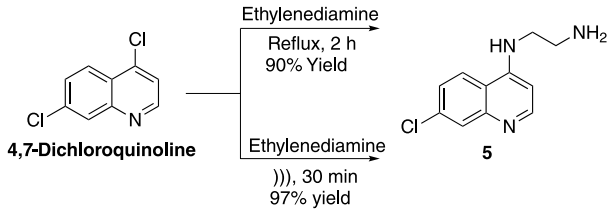

Scheme 1. Multigram scale synthesis of intermediate **5** by conventional heating and sonochemistry.

In fact, this kind of quinoline building block is very interesting to medicinal chemistry development as it allows the synthesis of chloroquine and primaquine analogs, as previously reported by our research group.[12,14] In order to continue our studies on potential anticancer molecules based on the structure of these two antimalarials, substituted thiourea **7** was synthesized from **5** according to Scheme 2. Firstly, benzoyl isothiocyanate was synthesized *in situ* by adding benzoyl chloride, dropwise, over 5 min, to a solution of NH_4SCN in acetone. After 30 min, a solution of intermediate **5** in acetone was quickly added to the reaction mixture and refluxed for 2 h to afford intermediate **6a** as the major product and amide **6b**, from the reaction of benzoyl chloride with **5**, as a side-product. The mixture was poured over ice and crude product **6a** was submitted to hydrolysis in methanol and aqueous NaOH (1 M) to afford crude key intermediate **7**, after extraction with ethyl acetate. Finally, thiazoles **1a-1g** were synthesized from the reaction of **7** with various 2-bromoacetophenones (**8a-8g**) in acetone under reflux for 30 min. The target products precipitated in the reaction medium as hydrobromide salts, were filtered, washed with acetone, and dried under high vacuum. The global yields for this synthetic route varied from 20 to 25% (Scheme 2).

The synthesized compounds were fully characterized by ^1H and ^{13}C NMR with the help of 2D homonuclear correlation spectroscopy (COSY), heteronuclear single quantum coherence (HSQC), and heteronuclear multiple bond correlation (HMBC) analysis, HRMS (ESI-TOF) and IR. All spectral data are in full agreement with the proposed structures. As an example, the ^1H NMR spectrum (400.00 MHz, MeOD) of compound **1g** shows the hydrogen

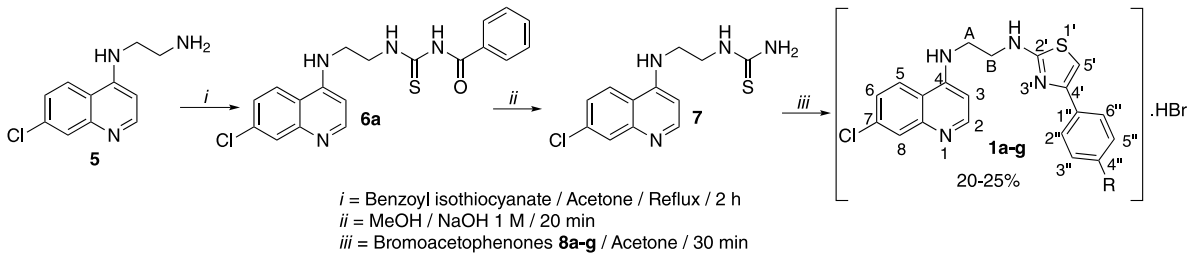

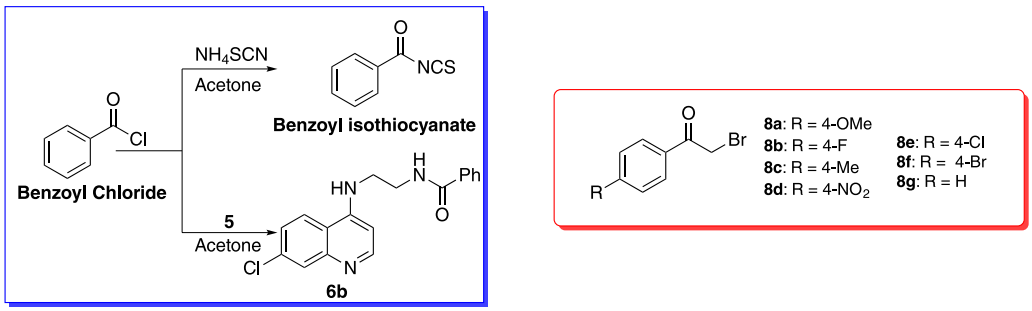

Scheme 2. Synthetic pathway to the quinoline-thiazole hybrids **1a-1g**. (*i*) Benzoyl isothiocyanate, acetone, reflux, 2 h; (*ii*) MeOH, NaOH(aq.) 1 M, r.t., 20 min; (*iii*): bromoacetophenones **8a-8g**, acetone, r.t., 30 min.

signals from the quinoline nucleus in δ 8.33 ppm (d, *J* 7.2 Hz, 1H, H2), 7.99 ppm (d, *J* 9.1 Hz, 1H, H5), 7.66 ppm (d, *J* 1.8 Hz, 1H, H8) and 7.00-6.95 ppm (m, 2H, H6 and H3). The phenyl ring hydrogens signals appear at 7.68 ppm (dd, *J* 8.2, 1.4 Hz, 2H, H2'') and 7.38-7.29 ppm (m, 3H, Ph). Finally, the characteristic thiazolic hydrogen H5' appears at 6.78 ppm (s, 1H, H5'). The main signals identified in the ^{13}C spectrum of substance **1g** are the thiazolic carbons C2' (171.5 ppm) and C5' (102.6 ppm); and the quinolinic carbons C2, C3, and C4 at 143.7, 99.9, and 158.0 ppm, respectively. It is also interesting to mention that the correlation of Hb with C2' and Ha with C4 ($^3J_{C\text{-}H}$) observed in the HMBC spectrum helped us to assign the hydrogens in the methylene groups at 3.91 ppm (m, 2H, Hb) and 3.84 (m, 2H, Ha) and their respective carbons at 43.4 (Cb) and 46.7 ppm (Ca). In the IR spectrum, the two N–H stretching vibrations at 3273 and 3202 cm^{-1}, besides the C=N and aliphatic C–N stretching bands at 1612 and 1215 cm^{-1}, respectively, stand out. Finally, HRMS (ESI-TOF) shows *m/z* 381.0924 ([M + H]$^+$, 100%; calcd. 381.0941).

Biology

The cytotoxic potential of the synthesized quinoline-thiazole hybrids **1a-1g** (Figure 4) was evaluated using the MTT assay. This assay has been widely used since its introduction by Mosmann in 1983[20] and became almost ubiquitous as a preliminary cell viability and cytotoxicity screening, providing quick and reproducible results.[31]

Substances **1a-1g** were assessed against four leukemia cell lines, Kasumi-1, KG-1, HL-60, and K562, the only cell line expressing the Philadelphia chromosome. The results are summarized in Tables 1 and 2.

In general, all compounds displayed high cytotoxicity against all tested cell lines, even though they were not as potent as the standard drug doxorubicin. However, it should

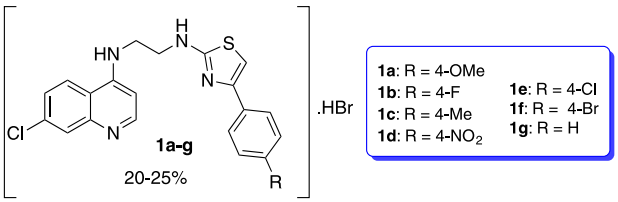

Figure 4. Quinoline-thiazole hybrids **1a-1g**.

be mentioned that all compounds seemed to be more potent against the Philadelphia chromosome-containing cell K562 (Chronic Myeloid Leukemia, CML), with all compounds, except **1d**, displaying better selectivity index (SI) than doxorubicin towards this cell line. Moreover, compounds **1a**, **1c**, and **1g** exhibited the most interesting results, being only two-fold less potent than doxorubicin, while keeping a higher selectivity index.

Molecular docking

It is widely known that the abnormal Philadelphia Chromosome carries the BCR-ABL gene, a potent oncogene that encodes the BCR-ABL protein, a tyrosine kinase that plays an important role in the pathogeneses of CML.[6,32] The BCR-ABL1 Tyrosine Kinase is the molecular target of many marketed drugs such as imatinib, ponatinib, dasatinib, and bosutinib.[32] Therefore, to investigate possible mechanisms of anticancer action of the synthesized quinoline-thiazole hybrids (**1a-1g**), we performed molecular docking simulations with the BCR-ABL1 Tyrosine Kinase (PDB 3QRJ)[21] using AutoDock Vina software.[22,23] This software performs the search for the binding modes of the ligands to the receptor by successive steps consisting of mutations in the structure of the docked molecule, followed by a local minima optimization using the Broyden-Fletcher-Goldfarb-Shanno (BFGS) *quasi*-Newton method.[33] The mutations in the structures of

Table 1. Cytotoxic activity expressed as IC_{50} (95% CI) of the quinoline-thiazole hybrids **1a-1g** against four leukemia cell lines and normal fibroblasts (L929), with doxorubicin (Dox) as the standard drug, obtained using nonlinear regression for all cell lines from three independent experiments

Compound	IC_{50} / μM				
	HL60	K562	KASUMI-1	KG-1	L929
1a	8.56 (7.21-10.16)	1.08 (0.76-1.55)	3.02 (2.41-3.78)	1.69 (1.31-2.17)	5.45 (4.41-6.72)
1b	7.99 (7.01-9.09)	1.49 (1.15-1.92)	4.72 (3.67-3.07)	2.96 (2.37-3.68)	7.06 (5.67-8.79)
1c	3.93 (3.19-4.85)	1.11 (0.79-1.55)	3.72 (2.79-4.95)	2.55 (2.05-3.14)	5.06 (3.96-6.46)
1d	3.29 (2.98-3.64)	1.51 (1.26-1.81)	3.06 (2.47-3.78)	2.85 (2.38-3.39)	2.85 (2.66-3.05)
1e	9.81 (7.82-12.30)	1.66 (1.36-2.03)	5.52 (4.77-6.39)	3.89 (3.20-4.73)	6.01 (5.26-6.90)
1f	8.89 (7.55-10.47)	2.12 (1.71-2.64)	3.46 (2.67-4.48)	5.19 (4.51-5.95)	11.20 (9.71-12.92)
1g	5.48 (4.38-6.86)	1.17 (0.95-1.46)	3.82 (3.38-4.31)	2.81 (2.24-3.50)	6.46 (5.25-7.93)
Dox	0.02	0.49	0.13	0.11	1.72

IC_{50}: half maximal inhibitory concentration; CI: confidence interval.

Table 2. Selectivity index calculated for compounds **1a-1g** and doxorubicin (Dox)

Compound	Selectivity index (L929 / tumoral cell line)			
	HL60	K562	Kasumi-1	KG-1
1a	0.64	5.02	1.80	3.22
1b	0.88	4.75	1.50	2.39
1c	1.29	4.57	1.36	1.99
1d	0.87	1.89	0.93	1.00
1e	0.61	3.62	1.09	1.55
1f	1.26	5.27	3.24	2.16
1g	1.18	5.50	1.69	2.30
Dox	86	3.51	13.23	15.63

the ligands are characterized by the change in the torsion of the active rotatable bonds (specifically the σ bonds, except for the amide bond in rebastinib), as well as its position and orientation in the active site. One limitation of using this conformational search strategy is that it does not change the bond distances and valence angles. To ensure that we are using consistent chemical structures of the ligands in the docking simulations, with reliable geometries, we started by performing a full structure optimization of each ligand at the quantum-chemical DFT method, B3LYP/6-31+G*. In the BFGS method, the values of the scoring functions and their gradients are used in the local minima optimization.[22] Vina searches the binding modes corresponding to the minima energy points during the optimization steps in trying to minimize the scoring function. This ultimately depends on the type of intra- and intermolecular interactions between atoms separated by, at least, three consecutive covalent bonds, and their distances. These functions are inspired by the X-score, used to calculate the binding score between a protein and a ligand.[34] The Vina uses the following scoring function weights and terms: –0.0356 for $gauss_1$, –0.00516 for $gauss_2$, 0.840 for repulsion, –0.0351 for hydrophobic, –0.587 for hydrogen bonding, and 0.0585 for N_{rot}. The first three terms are used to compute steric interactions and N_{rot} refers to the number of active rotatable bonds between heavy atoms in the ligand. These are used in a set of equations comprehensively presented in the seminal work that launched AutoDock Vina by Trott and Olson.[22]

The molecular target (BCR-ABL1 Tyrosine Kinase, under PDB code 3QRJ) was chosen since it has a mutation at the Thr315 amino acid residue, which is an essential residue for stabilizing the active conformation. Its replacement by the isoleucine (T315I) residue prevents conformational changes to the inactive form, conferring resistance, as seen for first and second-generation BCR-ABL tyrosine kinase inhibitors.[35] In addition, the co-crystallized ligand of the BCR-ABL1 Tyrosine Kinase, rebastinib, is a quinoline derivative and, thus, structurally analog to the series of synthetic compounds herein reported. This tinib is under investigation and used in trials for the treatment of Chronic Myeloid Leukemia. It is a non-competitive conformational control inhibitor, able to overcome T315I mutation.[36] We started by validating our docking protocol by superimposing the lowest-energy docked pose to the co-crystallized structure of rebastinib extracted from the ligand-protein complex (PDB ID: 3QRJ) (Figure 5), obtaining a low value of computed root-mean-square deviation (RMSD) of 0.0570 Å (Figure 5).[22]

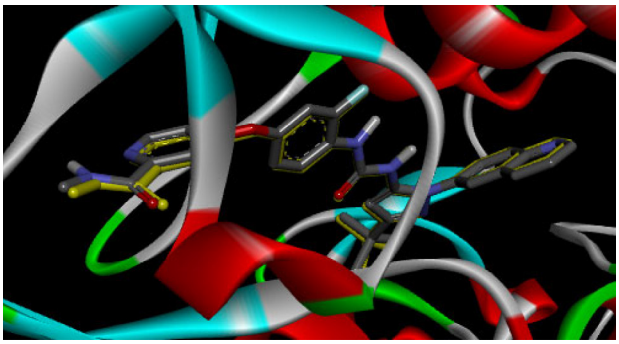

Figure 5. Superimposition of the co-crystallized ligand rebastinib (in yellow) and its redocked ligand at the human ABL1 kinase domain T315I mutant enzyme.

All quinoline-thiazole hybrids (**1a-1g**) and rebastinib were submitted to the molecular docking calculations at the human abl1 kinase domain of BCR-ABL1. For the synthesized compounds (**1a-1g**), the ligand-receptor interaction energy ranged from –7.2 to –8.9 kcal mol^{-1}. For rebastinib was –17.3 kcal mol^{-1} (Table 3). These findings suggest that these compounds are able to interact with the active site of the enzyme.

Table 3. Interaction energies of thiazole-containing 4-amino-quinolines (**1a-1g**) and rebastinib against Bcr-Abl1 tyrosine kinase (3QRJ)

Compound	Interaction energy / (kcal mol^{-1})
Rebastinib	–17.3
1a	–8.8
1b	–8.8
1c	–8.8
1d	–8.1
1e	–8.4
1f	–7.2
1g	–8.9

Docking of rebastinib showed extensive hydrogen and π interactions (Figure 6). The carboxamide-substituted pyridine ring established hydrogen bonds with the Met318 amino acid residue. It is reported that the hydrogen bond

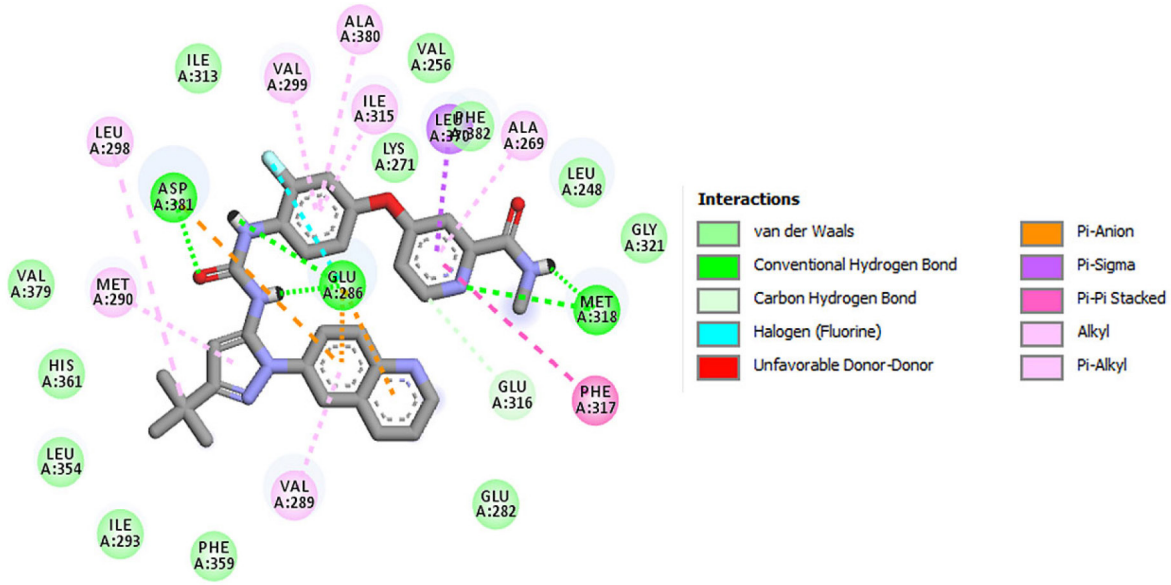

Figure 6. Docking pose of rebastinib (2D) in the binding site of BCR-ABL1 tyrosine kinase enzyme.

between a nitrogen atom and the backbone amide of Met318 is a characteristic feature of the binding mode of this class of inhibitors.[21,37] Urea nitrogen atoms also formed key hydrogen bonds with Glu286. An extra hydrogen bond was detected between the urea carbonyl and the amino group of Asp381. As seen for bosutinib, erlotinib, and gefitinib, π interactions occurred between the pyridine ring, Leu370, and Ala269.[38] Additional π interactions were established between the quinoline ring with Val289, Asp381, and Glu286; phenyl ring and Val299, Ala380 and Ile315, pyridine ring and Phe317 and Phe382.

For all the synthesized thiazole-containing 4-aminoquinolines (**1a-1g**), we also detected extensive π interactions and hydrogen bonds occurring between the aminoquinoline moiety and the amino acids from the target binding site (Figure 7), suggesting that these compounds are able to inhibit BCR-ABL1 if they reach its active site. The characteristic hydrogen bond with Met318 was detected only for compounds **1a** and **1d**. Glu286 performed hydrogen bonds with the compounds **1a**, **1d**, and **1e**, similar to rebastinib. π interactions with Leu370 and Ala269 residues were found in the enzyme complex with the compounds **1a**, **1d**, and **1e**, also detected for rebastinib, and described for bosutinib, erlotinib, and gefitinib.[35] An additional hydrogen bond between rebastinib and Asp381 was formed and also observed with the secondary amine of compounds **1a**, **1c**, and **1d**. Val281, Val299, Asp381, Glu286, Ala380, Ile315, Phe317, and Phe382 residues were involved in additional π interactions with rebastinib, and frequently detected in all aminoquinoline derivatives (**1a-1g**) complexes with the kinase.

Conclusions

We synthesized seven new cytotoxic quinoline-thiazole hybrids through a fast, easy, and reproducible procedure. All compounds exhibited interesting cytotoxic activity against four leukemia cell lines (HL-60, K562, Kasumi-1, KG-1) and normal fibroblasts (L929). Results against the K562 cell line were remarkable, with all compounds, except **1d**, exhibiting a higher SI when compared to doxorubicin. Docking studies suggest that all the synthesized compounds are able to interact with the BCR-ABL1 tyrosine kinase enzyme, highlighting compounds **1a** and **1d**, which established a key interaction with Met318 residue. The high affinity for BCR-ABL1 tyrosine kinase enzyme demonstrated by **1a** and **1d**, in addition to the cytotoxic effect in the MTT assay, propose that these 4-aminoquinolines derivatives are potential leads in the development of new anticancer agents.

Supplementary Information

All spectral data are available as supplementary data to this article free of charge at http://jbcs.sbq.org.br as PDF file.

Acknowledgments

The authors thank UFF, FAPERJ, CNPq, CAPES, and Farmanguinhos/FIOCRUZ for their support. We wish to thank FAPERJ, CNPq, and CAPES for their research fellowships.

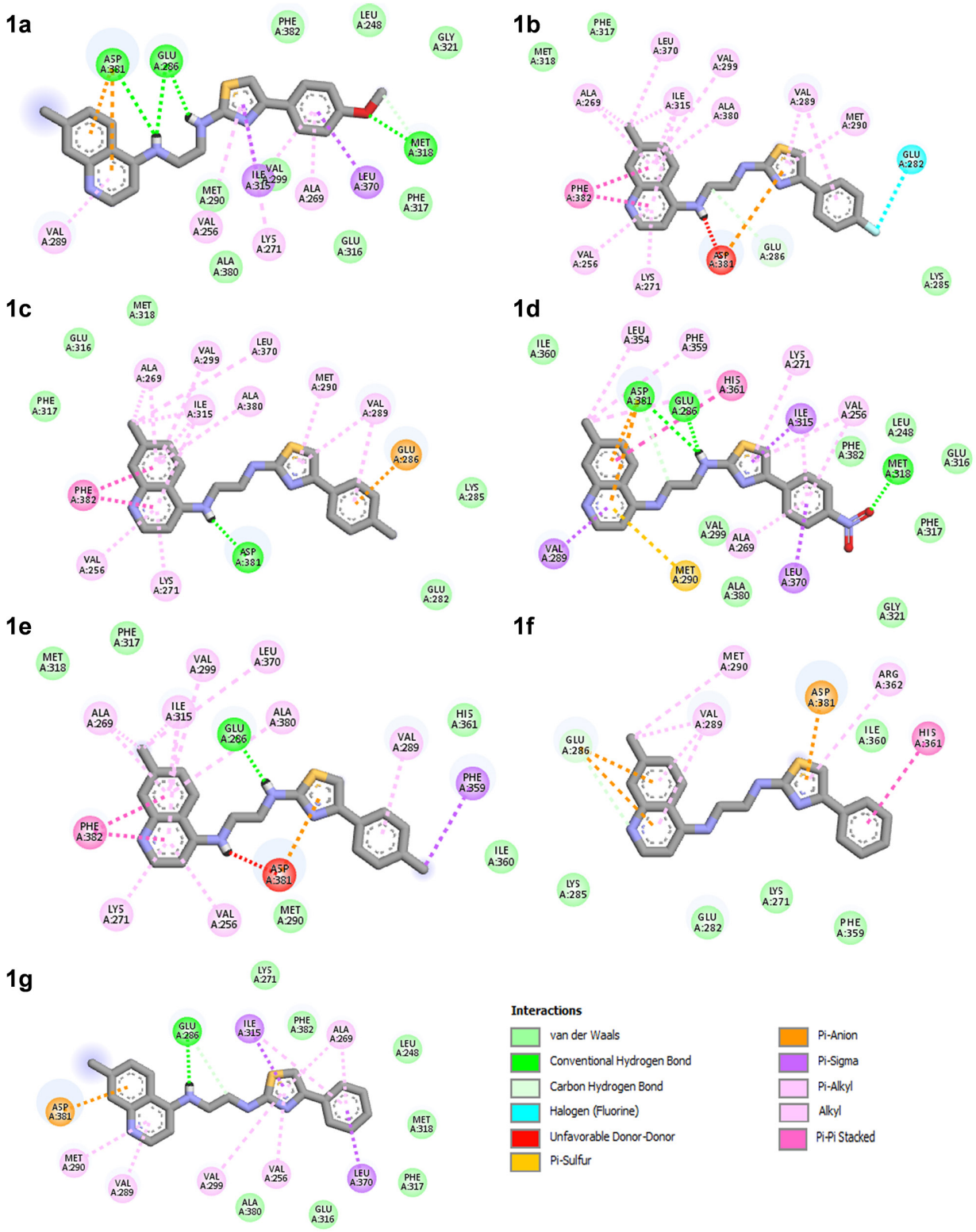

Figure 7. The docking pose of thiazole-containing 4-aminoquinolines (**1a-1g**) in the binding site of Bcr-Abl1 tyrosine kinase.

Author Contributions

Victor Facchinetti was responsible for the investigation of the synthesis, writing original draft, writing review and interpreting the results; Karoline C. L. Aboud for the investigation of the synthesis; Thatyana R. A. Vasconcelos and Marcus Vinícius N. de Souza for the conceptualization, supervision, project administration, writing original draft, writing review; Claudia Regina B. Gomes for the

investigation of the synthesis and writing review; Guilherme G. C. de Carvalho, Carlos Roberto K. Paier for the investigation of the biological activity; Claudia do Ó Pessoa for the investigation of the biological activity, writing original draft, interpreting the results and project administration; Anne Caroline C. Gomes and Rodolfo G. Fiorot were responsible for the conceptualization, investigation, and data curation of the molecular docking studies, for writing original draft and writing review.

References

1. International Agency for Research on Cancer, *Cancer Tomorrow*, https://gco.iarc.fr/tomorrow, accessed in August 2023.
2. Leukemia and Lymphoma Society, *Facts and Statistics Overview*, https://www.lls.org/facts-and-statistics/facts-and-statistics-overview/facts-and-statistics, accessed in August 2023.
3. Columbia University, *Leukemia Classifications*, https://cancer.columbia.edu/leukemia-classifications, accessed in August 2023.
4. American Cancer Society, *Cancer News and Stories*, https://www.cancer.org/latest-news/new-cancer-drug-approvals-from-2017.html, accessed in August 2023.
5. Baudino, T. A.; *Curr. Drug Discovery Technol.* **2015**, *12*, 3. [Crossref]
6. Nowell, P. C.; *J. Clin. Invest.* **2007**, *117*, 2033. [Crossref]
7. Tseng, C. H.; Chen, Y. L.; Lu, P. J.; Yang, C. N.; Tzeng, C. C.; *Bioorg. Med. Chem*. **2008**, *16*, 3153. [Crossref]
8. Ai, Y.; Liang, Y. J.; Liu, J. C.; He, H. W.; Chen, Y.; Tang, C.; Yang, G. Z.; Fu, L. W.; *Eur. J. Med. Chem*. **2012**, *47*, 206. [Crossref]
9. Jain, S.; Chandra, V.; Jain, P. K.; Pathak, K.; Pathak, D.; Vaidya, A.; *Arabian J. Chem.* **2019**, *12*, 4920. [Crossref]
10. Kashyap, S. J.; Garg, V. K.; Sharma, P. K.; Kumar, N.; Dudhe, R.; Gupta, J. K.; *Med. Chem. Res*. **2012**, *21*, 2123. [Crossref]
11. Cullis, C.; Granger, K.; Guo, J.; Hirose, M.; Li, G.; Mizutani, M.; Vos, T. J.; *WO 2012/021615 A1*, **2012**.
12. Bispo, M. L. F.; Alcantara, C. C.; Moraes, M. O.; Pessoa, C. O.; Rodrigues, F. A. R.; Kaiser, C. R.; Wardell, S. M. S. V.; Wardell, J. L.; de Souza, M. V. N.; *Monatsh. Chem*. **2015**, *146*, 2041. [Crossref]
13. Reis, R. R.; Azevedo, E. C.; de Souza, M. C. B. V.; Ferreira, V. F.; Montenegro, R. C.; Araújo, A. J.; Pessoa, C.; Costa-Lotufo, L.V.; de Moraes, M. O.; Filho, J. D. B. M.; de Souza, A. M. T.; de Carvalho, N. C.; Castro, H. C.; Rodrigues, C. R.; Vasconcelos, T. R. A.; *Eur. J. Med. Chem.* **2011**, *46*, 1448. [Crossref]
14. Pinto, L. S. S.; de Souza, M. V. N.; Kaiser, C. R.; Wardell, J. L.; Wardell, S. M. S. V.; *Lett. Drug Des. Discovery* **2018**, *2*, 113. [Crossref]
15. Ghorab, M. M.; Al-Said, M. S.; Arafa, R. K.; *Acta Pharm.* **2014**, *64*, 285. [Crossref]
16. Choi, A. R.; Kim, J. H.; Woo, Y. H.; Kim, H. S.; Yoon, S.; *Anticancer Res.* **2016**, *36*, 1641. [PubMed]
17. Rodrigues, F. A. R.; Bomfim, I. S.; Cavalcanti, B. C.; Pessoa, C.; Wardell, J. L.; Wardell, S. M. S. V.; Pinheiro, A. C.; Kaiser, C. R.; Nogueira, T. C. M.; Low, J. N.; Gomes, L. R.; de Souza, M. V. N.; *Bioorg. Med. Chem. Lett.* **2014**, *24*, 934. [Crossref]
18. Fletcher, S.; Keaney E. P.; Cummings, C. G.; Blaskovich, M. A.; Hast, M. A.; Glenn, M. P.; Chang, S. Y.; Bucher, C. J.; Floyd, R. J.; Katt, W. P.; Gelb, M. H.; Van Voorhis, W. C.; Beese, L. S.; Sebti, S. M.; Hamilton, A. D.; *J. Med. Chem.* **2010**, *53*, 6867. [Crossref]
19. Skehan, P.; Storeng, R.; Scudiero, D.; Monks, A.; McMahon, J.; Vistica, D.; Warren, J. T.; Bodesch, H.; Kenney, S.; Boyd, M. R.; *J. Natl. Cancer Inst.* **1990**, *82*, 1107. [Crossref]
20. Mosmann, T.; *J. Immunol. Methods* **1983**, *65*, 55. [Crossref]
21. Chan, W. W.; Wise, S. C.; Kaufman, M. D.; Ahn, Y. M.; Ensinger, C. L.; Haack, T.; Hood, M. M.; Jones, J.; Lord, J. W.; Lu, W. P.; Miller, D.; Patt, W. C.; Smith, B. D.; Petillo, P. A.; Rutkoski, T. J.; Telikepalli, H.; Vogeti, L.; Yao, T.; Chun, L.; Clark, R.; Evangelista, P.; Gavrilescu, L. C.; Lazarides, K.; Zaleskas, V. M.; Stewart, L. J.; Van Etten, R. A.; Flynn, D. L.; *Cancer Cell* **2011**, *19*, 556. [Crossref]
22. Trott, O.; Olson, A. J.; *J. Comput. Chem.* **2010**, *31*, 455. [Crossref]
23. *AutoDock Vina*, version 1.2.0; Molecular Graphics Lab, The Scripps Research Institute, USA, 2009.
24. *MarvinSketch*, Marvin version 20.11; Chem Axon, Hungary, 2020. [Link] accessed in August 2023
25. Frisch, M. J.; Trucks, G. W.; Schlegel, H. B.; Scuseria, G. E.; Robb, M. A.; Cheeseman, J. R.; Scalmani, G.; Barone, V.; Mennucci, B.; Petersson, G. A.; Nakatsuji, H.; Caricato, M.; Li, X.; Hratchian, H. P.; Izmaylov, A. F.; Bloino, J.; Zheng, G.; Sonnenberg, J. L.; Hada, M.; Ehara, M.; Toyota, K.; Fukuda, R.; Hasegawa, J.; Ishida, M.; Nakajima, T.; Honda, Y.; Kitao, O.; Nakai, H.; Vreven, T.; Montgomery Jr., J. A.; Peralta, J. E.; Ogliaro, F.; Bearpark, M.; Heyd, J. J.; Brothers, E.; Kudin, K. N.; Staroverov, V. N.; Kobayashi, R.; Normand, J.; Raghavachari, K.; Rendell, A.; Burant, J. C.; Iyengar, S. S.; Tomasi, J.; Cossi, M.; Rega, N.; Millam, J. M.; Klene, M.; Knox, J. E.; Cross, J. B.; Bakken, V.; Adamo, C.; Jaramillo, J.; Gomperts, R.; Stratmann, R. E.; Yazyev, O.; Austin, A. J.; Cammi, R.; Pomelli, C.; Ochterski, J. W.; Martin, R. L.; Morokuma, K.; Zakrzewski, V. G.; Voth, G. A.; Salvador, P.; Dannenberg, J. J.; Dapprich, S.; Daniels, A. D.; Farkas, Ö.; Foresman, J. B.; Ortiz, J. V.; Cioslowski, J.; Fox, D. J.; *Gaussian 09*, Rev. D.01; Gaussian Inc, Wallingford, Connecticut, USA, 2009.
26. Becke, A. D.; *J. Chem. Phys.* **1993**, *98*, 5648. [Crossref]
27. *BIOVIA*, version 2019; Dassault Systèmes, San Diego, USA, 2019.
28. Pinto, L. S.; de Souza, M. V. N.; *Curr. Green. Chem.* **2018**, *5*, 104. [Crossref]

29. Costa, G. O.; Facchinetti, V.; Bezerra, M. S.; Gomes, C. R. B.; de Souza, M. V. N.; *Braz. J. Dev.* **2021**, *7*, 48138. [Crossref] accessed in April 2023
30. de Souza, M. V. N.; Pais, K. C.; Kaiser, C. R.; Peralta, M. A.; Ferreira, M. L.; Lourenço, M. C.; *Bioorg. Med. Chem.* **2008**, *17*, 1474. [Crossref]
31. Supino, R. In *In Vitro Toxicity Testing Protocols*; O'Hare, S.; Atterwill, C. K., eds.; Springer: New Jersey, USA, 1995, p.137. [Crossref]
32. Teng, M.; Luskin, M. R.; Cowan-Jacob, S. W.; Ding, Q.; Fabbro, D.; Gray, N. S.; *J. Med. Chem.* **2022**, *65*, 7581. [Crossref]
33. Nocedal, J.; Wright, S. J. In *Numerical Optimization*; Glynn, P.; Robinson S. M., eds.; Springer Series in Operations Research: Berlin, Germany, 1999.
34. Wang, R.; Lai, L.; Wang, S.; *J. Comput-Aided Mol. Des.* **2002**, *16*, 11. [Crossref]
35. Rossari, F.; Minutolo, F.; Orciuolo, E.; *J. Hemat. Oncol.* **2018**, *11*, 84. [Crossref]
36. Eide, C. A.; Adrian, L. T.; Tyner, J. W.; Mac Partlin, M.; Anderson, D. J.; Wise, S. C.; Smith, B. D.; Petillo, P. A.; Flynn, D. L.; Deininger, M. W.; O'Hare, T.; Druker, B.; *J. Cancer Res.* **2011**, *71*, 3189. [Crossref]
37. Levinson, N. M.; Boxer, S. G.; *PloS One* **2012**, *7*, e29828. [Crossref]
38. Zhou, Y.; Portelli, S.; Pat, M.; Rodrigues, C. H. M.; Nguyen, T. B.; Pires, D. E. V.; Ascher, D. B.; *Comput. Struct. Biotechnol. J.* **2021**, *19*, 5381. [Crossref]

Submitted: May 18, 2023
Published online: August 17, 2023